GEOPHYSICAL RESEARCH LETTERS, VOL. 33, L21S03, doi:10.1029/2006GL026881, 2006

Uptake and sequestration of atmospheric CO_2 in the Labrador Sea deep convection region

M. D. DeGrandpre,[1] A. Körtzinger,[2] U. Send,[3] D. W. R. Wallace,[2] and R. G. J. Bellerby[4,5]

Received 11 May 2006; revised 6 September 2006; accepted 11 September 2006; published 13 October 2006.

[1] The Labrador Sea is an important area of deep water formation and is hypothesized to be a significant sink for atmospheric CO_2 to the deep ocean. Here we examine the dynamics of the CO_2 system in the Labrador Sea using time-series data obtained from instrumentation deployed on a mooring near the former Ocean Weather Station Bravo. A 1-D model is used to determine the air-sea CO_2 uptake and penetration of the CO_2 into intermediate waters. The results support that mixed-layer pCO_2 remained undersaturated throughout most of the year, ranging from 220 μatm in mid-summer to 375 μatm in the late spring. Net community production in the summer offset the increase in pCO_2 expected from heating and air-sea uptake. In the fall and winter, cooling counterbalanced a predicted increase in pCO_2 from vertical convection and air-sea uptake. The predicted annual mean air to sea flux was 4.6 mol m^{-2} yr^{-1} resulting in an annual uptake of 0.011 ± 0.005 Pg C from the atmosphere within the convection region. In 2001, approximately half of the atmospheric CO_2 penetrated below 500 m due to deep convection. **Citation:** DeGrandpre, M. D., A. Körtzinger, U. Send, D. W. R. Wallace, and R. G. J. Bellerby (2006), Uptake and sequestration of atmospheric CO_2 in the Labrador Sea deep convection region, *Geophys. Res. Lett.*, *33*, L21S03, doi:10.1029/2006GL026881.

1. Introduction

[2] Observations [*Takahashi et al.*, 2002; *Skjelvan et al.*, 2005] and models [*McKinley et al.*, 2004] predict that high latitude surface waters are large sinks for atmospheric CO_2. In these mostly mesotrophic regions, moderate to strong summer time biological production is followed by fall and winter cooling – these processes, known as the biological and solubility pumps, act together to sustain seawater partial pressure of CO_2 (pCO_2) below atmospheric saturation for long periods or even maintain a perennial CO_2 sink [*Skjelvan et al.*, 2005]. In the Labrador Sea, a major deep water formation region, the atmospheric CO_2 that is taken up can be transported to great depths on short time scales. The total amount of CO_2 exported and its vertical distribution in the Labrador Sea may thus have global carbon cycle implications. Interannual variability in deep convection [*Lazier et al.*, 2002; *Avsic et al.*, 2006] and the predicted decline of thermohaline circulation in the anthropocene ocean [*Gregory et al.*, 2005] have the potential to alter the rate of CO_2 accumulation in the atmosphere. Deep convection redistributes anthropogenic CO_2 to intermediate depths where increased CO_2 levels decrease pH and increase $CaCO_3$ solubility [*Feely et al.*, 2004]. In spite of its potential importance in the global carbon cycle, few carbon-related measurement programs have been undertaken in the Labrador Sea. A long-term time-series station is visited annually in June by Bedford Institute of Oceanography near Ocean Weather Station Bravo (OWSB). Other research cruises have been short duration studies and very few CO_2-related data have been collected outside the summer season. We present here the first continuous observations of pCO_2 in the Labrador Sea. The data span a full annual cycle between June 2000 and June 2001. A 1-D box model, constrained by the pCO_2 data, is used to examine sources of variability, estimate air-sea uptake, and determine the vertical distribution of atmospheric CO_2.

2. Methods

2.1. Measurements

[3] A mooring was deployed on 3 June 2000 at 56.54°N, 52.64°W, near the former location of OWSB in the south central Labrador Sea. The mooring was recovered on 5 June 2001. An autonomous pCO_2 sensor (SAMI-CO_2 [*DeGrandpre et al.*, 1995]) was located at 13 m and 14 CTD sensors were distributed between 13 m and 3300 m in the water column. Measurements of pCO_2, temperature and salinity were made at 2-hour intervals throughout the entire 12-month deployment period. On 12 July 2000, the surface flotation detached in a storm and the pCO_2 sensor sank to ~180 m depth. The sensor time-series therefore comprises measurements in both surface and subsurface waters. Total alkalinity (A_T) and dissolved inorganic carbon (DIC) were measured on 4 samples within the surface mixed-layer on 3 June 2000 and 6 June 2001 [P. Jones, unpublished]. These results were used with the CO_2 thermodynamic constants given by *Dickson and Millero* [1987] to calculate pCO_2 at the mooring site for validation of the in situ pCO_2. Based on comparisons with these data, a 20 μatm positive offset and 0.19 μatm d^{-1} drift correction were applied to the SAMI-CO_2 data. The drift correction was applied starting in late October when a downward drift appeared to initiate based on examination of the raw (light intensity) data. We believe that the offset and drift are due to calibration problems prior to deployment and precipitation of the indicator in cold water conditions, respectively. With these corrections, the SAMI data compare

[1]Department of Chemistry, University of Montana, Missoula, Montana, USA.
[2]Marine Biogeochemie, Leibniz-Institut für Meereswissenschaften, Kiel, Germany.
[3]Scripps Institution of Oceanography, University of California, San Diego, La Jolla, California, USA.
[4]Bjerknes Centre for Climate Research, University of Bergen, Bergen, Norway.
[5]Also at Geophysical Institute, University of Bergen, Bergen, Norway.

0094-8276/06/2006GL026881

to within ±5 μatm of the shipboard data collected before and after deployment (n = 4).

2.2. Model

[4] A 1-D vertical biogeochemical model with air-sea gas exchange, net community production and complete CO_2 thermodynamics was used to predict pCO_2. Similar models were used by *Baehr and DeGrandpre* [2004] and *DeGrandpre et al.* [2004]. Others have interpreted variability using 1-D models with reasonable success in the Labrador Sea [e.g., *Tian et al.*, 2004]. The model mass balance equation is

$$H\frac{dDIC}{dt} = F_{GAS} + F_{NCP} + F_{ENT} \quad (1)$$

where H is the surface mixed-layer depth, $\frac{dDIC}{dt}$ is the rate of change of dissolved inorganic carbon (DIC) due to air-sea gas exchange (F_{GAS}), net community production (F_{NCP}) and vertical entrainment (F_{ENT}). Mixed-layer depth was estimated using the temperature and salinity data collected on the mooring. The surface mixed-layer was defined as the depth where $\Delta\sigma$ = 0.025 kg m^{-3} between the surface and measurement depth. This density criterium was selected by comparing mixed-layer estimates with visual inspection of the density time-series. In the model, subsurface water is mixed with surface water to the depth where $\Delta\sigma$ = 0.025 kg m^{-3}, keeping track of DIC by mass balance (F_{ENT}) (equation (1)). Recent measurements of DIC in water below ~130 m have consistently found values near 2150 μmol kg^{-1} in the Labrador Sea [Körtzinger et al. unpubl. from July 1997 and 1999; P. Jones unpubl. from June 2000 and 2001] and North Water [*Miller et al.*, 2002] so this value was used as the subsurface water end member. The initial DIC profile was estimated by interpolating between the deep end member and surface values at the beginning of the time-series (calculated to be 2125 μmol kg^{-1}). In the model, DIC was incremented for each flux term in equation (1) using a 1 hr time step. Mixed-layer pCO_2 was calculated using thermodynamic equations that give pCO_2 = f(DIC, A_T, T and S) [*Dickson and Millero*, 1987]. Herein, A_T was calculated using a salinity and temperature dependent relationship derived from A_T measured over the depth range 0–200 m [*Tait et al.*, 2000]. It was necessary to add 10 μmol kg^{-1} to the calculated A_T to obtain consistent end member values for the other parameters (i.e. pCO_2 = 370 μatm and DIC = 2150 μmol kg^{-1}), possibly due to uncertainty in the equilibrium constants used in the thermodynamic model [*Lee et al.*, 1996]. The calculated, corrected (+10 μmol kg^{-1}) A_T ranged from 2285 to 2305 μmol kg^{-1} over the deployment period.

[5] Air-sea gas exchange (F_{GAS}) was calculated using $F_{GAS} = k\ S\ \Delta pCO_2$ where k is the gas transfer velocity, S is the gas solubility and ΔpCO_2 is the pCO_2 difference across the air-sea interface. The gas transfer velocity was estimated using the wind-speed relationship from *Wanninkhof* [1992] for long-term averaged winds. Monthly averaged winds were obtained from the COADS time-series for 2000–2001 and interpolated on a 1 hr interval. Solubility was calculated using equations from *Weiss* [1974]. The atmospheric CO_2 mole fraction was obtained from the Alert station in northern Canada for 2000–2001 [cdiac.ornl.gov]. Net community production (F_{NCP}) was assumed to be proportional to the product of solar irradiance at the latitude of the mooring and phytoplankton biomass [*Bidigare et al.*, 1992]. The trends in phytoplankton biomass were assumed to follow the annual cycle shown by *Tian et al.* [2004]. NCP was set equal to zero at 180 m, i.e. no net respiration. The proportionality constant in the NCP model was constrained by the subsurface data (described below) and the *Takahashi et al.* [2002] pCO_2 climatology. A mean NCP of 4.3 mol carbon m^{-2} yr^{-1} was obtained using this approach which is ~40% of the estimated annual primary production [*Behrenfeld and Falkowski*, 1997] and somewhat lower than the 59% new production estimated by *Tian et al.* [2004] for the Labrador Sea.

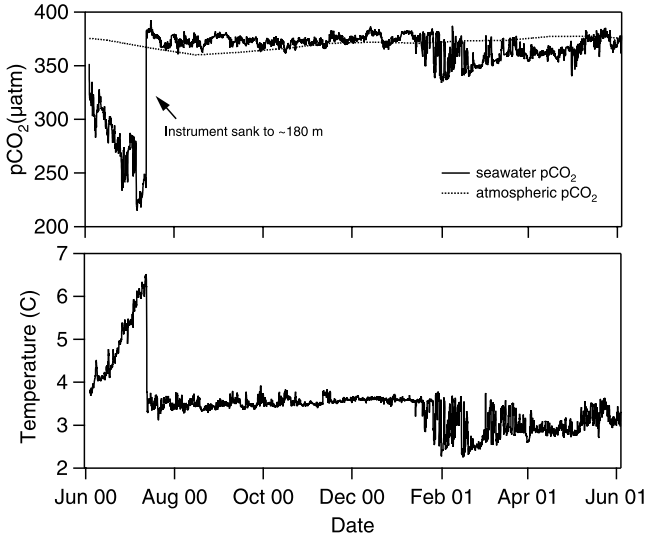

Figure 1. (top) Time-series of the CO_2 partial pressure (pCO_2) in seawater as measured by an autonomous pCO_2 sensor from a mooring in the south central Labrador Sea (56.54°N, 52.64°W); atmospheric CO_2 from the Alert station (dotted curve) is also shown. (bottom) Time-series of seawater temperature at the depth of the pCO_2 sensor.

3. Results and Discussion

3.1. Overview

[6] We first discuss the variability in the pCO_2 and temperature time-series. The model is then used to ascribe the variability to specific sources. The modeled mixed-layer pCO_2 is used to estimate the annual air-sea CO_2 flux in the Labrador Sea deep convection region and the subsequent distribution of atmospheric CO_2 in the water column.

3.2. Measurements

[7] Time-series of seawater pCO_2, atmospheric pCO_2, temperature and sensor depth are shown in Figures 1 and 2. From June to July, sea surface pCO_2 dropped from ~350 to 220 μatm while sea surface temperature increased by ~2.5°C. Without the heating, the pCO_2 decrease (ignoring air-sea CO_2 flux) would have been ~170 μatm. This drawdown was driven by the summer phytoplankton bloom, which typically peaks in early July [*Tian et al.*, 2004]. The deep time-series after the instrument sank (12 July) showed

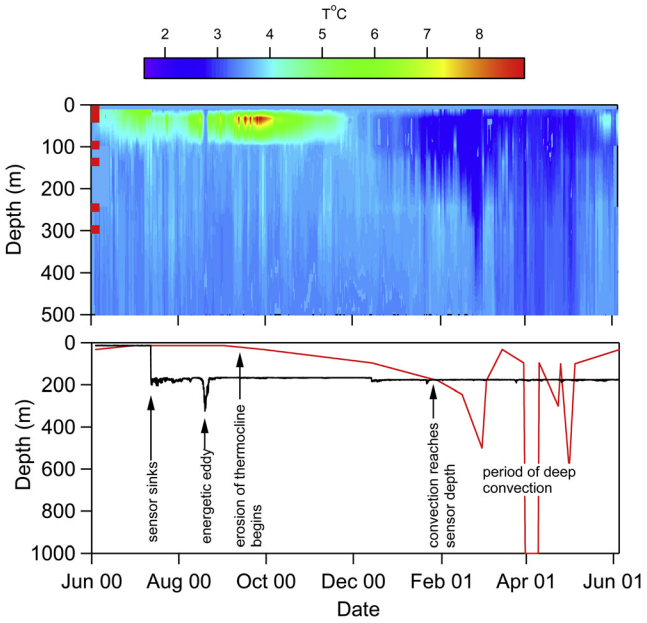

Figure 2. (top) Temperature contour time-series derived from CTD sensors deployed at depths shown with red squares on the y-axis. The contour data are only plotted to 500 m for clarity. Additional CTD data obtained at 506, 750, 999 and 1250 m found that convection reached a maximum of ~1000 m during 2001. (bottom) Interpolated mixed-layer depth (red) and sensor depth (black). Major events are indicated.

no significant upward or downward trend for ~6 months (mean value 374 ± 4 μatm) (Figure 1). On 20 August, the mooring was pushed downward to ~350 m for a short period by an energetic eddy (Figure 2) with no significant change in pCO_2 providing evidence that no vertical CO_2 gradients exist down to this depth. The ~40 μatm drop in late January corresponds to lower temperature water which suggests that the wintertime mixed layer had reached the sensor depth. The large fluctuations in pCO_2 that followed are likely due to advection of incompletely mixed waters before the onset of more vigorous convection. These fluctuations diminish by April suggesting that continued and more widespread convection erased any remaining horizontal gradients at the sensor depth. During this time and through the late spring, the pCO_2 and temperature at 180 m climbed back towards early winter values (Figure 1). The rapid decline of mixed layer depth due to development of a low salinity surface layer after peak convection [*Körtzinger et al.*, 2004; *Avsic et al.*, 2006] decouples the 180 m pCO_2 from the surface layer after early May. The increase in the deep pCO_2 towards early winter levels after this time may be due to lateral advection or by respiration of organic matter already exported from the surface production.

[8] The temperature time-series (Figure 2) and calculations by *Avsic et al.* [2006] show that convection reached ~1000 m during winter 2001. The interpolated mixed-layer depth reveals the erosion of the seasonal thermocline along with brief periods of deep mixing and rapid restratification (Figure 2).

3.3. Model Results

[9] In the model development, the observations at 180 m were used to constrain the modeled sea surface pCO_2. The modeled 180 m pCO_2 varied only with the small changes in temperature shown in Figure 1 until late January when the pCO_2 dropped by ~35–40 μatm. Figure 2 shows that the mixed-layer reached the sensor depth at this time. The mixed-layer water was lower in DIC (2140 compared to 2150 μmol kg^{-1}, Figure 3) and lower in temperature (2.6 compared to 3.6°C) causing the pCO_2 to drop significantly. To model the observed drop in pCO_2, the DIC of the surface water was constrained to 2140 ± 5 μmol kg^{-1}. With this DIC magnitude and uncertainty, the model predicted the observed drop in pCO_2 to within ~10 μatm. The modeled pCO_2 and DIC within the mixed-layer and at 180 m depth are shown in Figure 3 along with individual contributions from each flux term in equation 1. We use these results to evaluate the major processes controlling both pCO_2 and DIC over the annual cycle.

[10] Biological production drove the large pCO_2 decrease during the early summer months; however, the model did not predict the dynamics or the full magnitude of the drawdown (Figure 3, first panel). These inconsistencies may be due to patchy blooms and interannual differences in phytoplankton biomass, respectively. The model does reveal that biological production offset a pCO_2 increase due to air-sea uptake and heating. If the model net community production was set to zero, the pCO_2 would reach atmospheric saturation by late August due to heating and air-sea exchange.

[11] After the early summer bloom, the pCO_2 slowly increased towards atmospheric pCO_2 through the fall and winter, which is also clearly documented in the climatological pCO_2 (Figure 3). From late July to September, the increase in pCO_2 was driven by continued surface heating and CO_2 uptake from the atmosphere into the highly undersaturated surface waters. These processes overcame biological production which dropped to about one third of its peak value by mid-August (Figure 3, fourth panel). High rates of air-sea CO_2 exchange were sustained well after the peak in NCP because of the slow rate of pCO_2 equilibration with the atmosphere (CO_2 system buffering). After the peak in surface temperature in early September, convective mixing of subsurface water (Figure 2) with higher DIC, in addition to air-sea CO_2 uptake, increased pCO_2 but cooling significantly countered these processes. After late autumn, changes in DIC were reduced as pCO_2 approached atmospheric equilibrium and biological production dropped to near zero (Figure 3, fourth panel).

[12] During the latter portion of the time-series, the surface DIC continued to slowly climb towards the end member value (2150 μmol kg^{-1}) as convection and air-sea uptake continued (Figures 2 and 3). Surface mixed-layer pCO_2 increased in kind, finally approaching atmospheric saturation in late May (Figure 3). The predicted mixed-layer pCO_2 generally followed the *Takahashi et al.* [2002] climatology until April. Although biological production was significant, deep convection continued into late spring of 2001, with the mixed-layer reaching 600 m in early May and offsetting any loss of DIC due to net biological uptake (Figure 3, fourth panel). Convection episodically added DIC to the mixed-layer with some large spikes

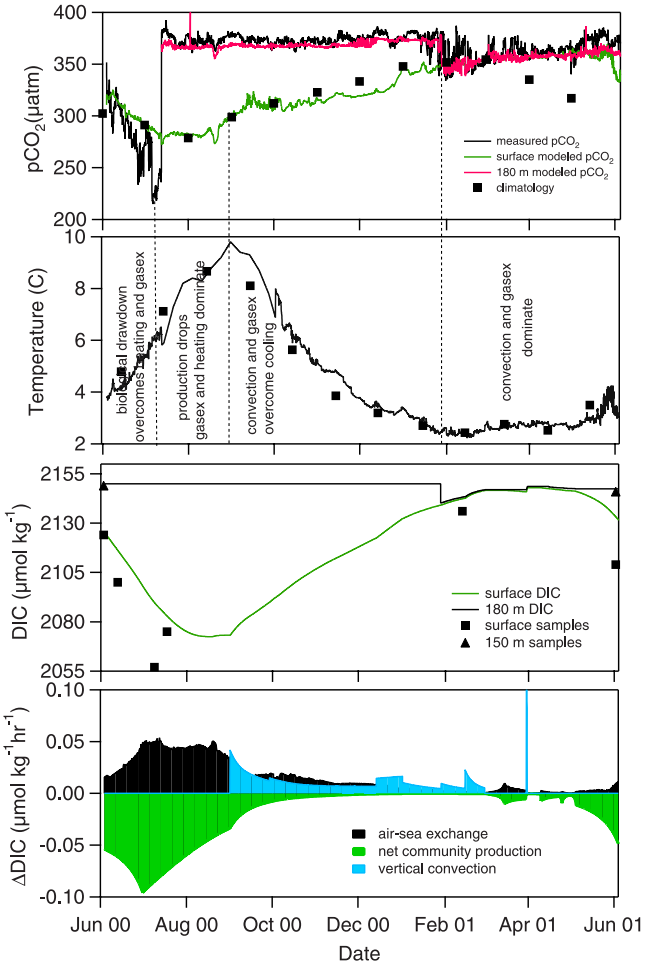

Figure 3. Time-series of measured and modeled pCO_2 for surface and deep (180 m) waters (first panel). The measured values at the surface are combined with the model data to estimate air-sea CO_2 fluxes. Also shown are the climatological pCO_2 values at the mooring site [*Takahashi et al.*, 2002]. Time-series of mixed layer temperature in the Labrador Sea (second panel). SST was obtained from satellite data when the mixed-layer depth was shallower than the 32 m temperature sensor (July–October). The sea surface temperature climatology is also shown (black squares) and indicate that the 2000–2001 period is representative of climatological conditions. Modeled time-series of dissolved inorganic carbon (DIC) in the mixed-layer and at 180 m depth (equivalent when the mixed-layer extended deeper than 180 m) (third panel). Discrete samples collected since 1997 used to constrain the model are shown for comparison (black symbols). Contributions from separate processes to the hourly change in DIC in the mixed-layer (fourth panel). Biological production is a loss of DIC and is therefore <0. The large spike in late March is a result of deep convection which increased the DIC by up to 0.26 μmol kg^{-1} over a short period.

(>0.2 μmol kg^{-1} hr^{-1}) when the mixed-layer deepened rapidly over a short period. A drawdown comparable to the pCO_2 climatology, but later in the spring, can be reproduced with a shallow MLD (<50 m) – therefore, these results suggest that pCO_2 levels in late spring are very sensitive to the duration of convection.

[13] Summarizing the DIC results in Figure 3 (fourth panel), the net contributions to changes in mixed-layer DIC over the annual period were 130 μmol kg^{-1} $year^{-1}$ for air-sea uptake, −180 μmol kg^{-1} $year^{-1}$ for NCP and 50 μmol kg^{-1} $year^{-1}$ for vertical convection – the relative contributions to DIC variability being 36% gas exchange, 50% NCP, and 14% convection.

3.4. Air-Sea CO_2 Uptake

[14] The model provides strong evidence that the mixed-layer pCO_2 remained significantly undersaturated for most of the year. These predictions are also supported by new observations (Körtzinger et al., unpubl.). Using the pCO_2 measurements from June 3 – July 12, 2000 and the surface modeled pCO_2 thereafter, the air-sea CO_2 flux ranged from −10.1 to +0.2 mol CO_2 m^{-2} yr^{-1} with an average annual uptake of −4.6 mol m^{-2} yr^{-1}. This flux is comparable to other areas of deep convection in the sub-Arctic seas in the North Atlantic estimated by *Skjelvan et al.* [2005] also using the *Wanninkhof* [1992] gas transfer rates. The uncertainty in our predicted flux based on the possible range of gas transfer rates is ∼50%, e.g. the flux is −2.4 mol m^{-2} yr^{-1} using the *Liss and Merlivat* [1986] gas transfer parameterization. The air-sea CO_2 flux is not sensitive to the timing nor depth of convection because mixing occurs between surface and sub-surface waters that are already close to atmospheric equilibrium. The model predicts that the air-sea flux decreases by only ∼10% if convection reaches 2000 m one month earlier (1 February).

[15] Using the area of deep convection estimated from figures given by *Lavender et al.* [2000] of 350 × 550 km^2, the modeled flux corresponds to a net uptake in the deep convection region of 0.011 ± 0.005 Pg carbon per year with the uncertainty originating from the gas transfer rate. Because most of the atmospheric CO_2 is taken up during the period of strong undersaturation prior to deep convection (Figure 3), it can then be sequestered into intermediate waters when deep convection occurs. In 2001, about half of the 0.011 Pg of atmospheric CO_2 was transported below 500 m and none below 1000 m, the deepest depth of convection. The ultimate fate of the atmospheric CO_2 is unknown but recent findings for convective buildup of the oxygen inventory in the Labrador Sea indicate that a major fraction of the atmospheric CO_2 gets rapidly entrained into the ocean interior [*Körtzinger et al.*, 2004].

[16] The results presented here provide important insights into the annual cycle of CO_2 in the Labrador Sea. The model assumes steady state conditions and ignores horizontal advection, however, and more realistic mesoscale physical and ecological modeling should be undertaken to verify our results. Studies are also currently underway to capture a full year of pCO_2 variability in the mixed-layer which can be compared to the modeled CO_2 from this study. An important future step will be to examine interannual variability in the air-sea flux in this important deep water formation region.

[17] **Acknowledgments.** We thank Cory Beatty for instrument preparation and data analysis, Jochen König and Tom Avsic for providing climatological data and Peter Jones, Robert Gershey, and Karsten Friis for providing DIC and A_T data. Insightful comments by the two reviewers were

appreciated. This work was supported by SFB 460 of the German Research Foundation which included a visiting scientist grant to MDD to the Institute for Marine Science in Kiel, Germany. We also acknowledge the financial support of the European Commission within the 6th Framework (EU FP6 CARBOOCEAN Integrated Project, contract 511176) and the U.S. National Science Foundation under OCE-0327274 (MDD).

References

Avsic, T., J. Karstensen, U. Send, and J. Fischer (2006), Interannual variability of newly formed Labrador Sea Water from 1997 to 2005, *Geophys. Res. Lett.*, doi:10.1029/2006GL026913, in press.

Baehr, M. M., and M. D. DeGrandpre (2004), In situ pCO_2 and O_2 measurements in a freshwater lake during turnover and stratification: Observations and a model, *Limnol. Oceanogr.*, *49*, 330–340.

Behrenfeld, M. J., and P. G. Falkowski (1997), Photosynthetic rates derived from satellite-based chlorophyll concentration, *Limnol. Oceanogr.*, *42*, 1–20.

Bidigare, R. R., B. B. Prézelin, and R. C. Smith (1992), Bio-optical models and the problems of scaling, in *Primary Productivity and Biogeochemical Cycles in the Sea*, edited by P. G. Falkowski and A. D. Woodhead, pp. 175–212, Springer, New York.

DeGrandpre, M. D., T. R. Hammar, S. P. Smith, and F. L. Sayles (1995), In situ measurements of seawater pCO_2, *Limnol. Oceanogr.*, *40*, 969–975.

DeGrandpre, M. D., R. Wanninkhof, W. R. McGillis, and P. G. Strutton (2004), A Lagrangian study of surface pCO_2 dynamics in the eastern equatorial Pacific Ocean, *J. Geophys. Res.*, *109*, C08S07, doi:10.1029/2003JC002089.

Dickson, A. G., and F. J. Millero (1987), A comparison of the equilibrium constants for the dissociation of carbonic acid in seawater media, *Deep Sea Res.*, *34*, 1733–1743.

Feely, R. A., et al. (2004), Impact of anthropogenic CO_2 on the $CaCO_3$ system in the oceans, *Science*, *305*, 362–366.

Gregory, J. M., et al. (2005), A model intercomparison of changes in the Atlantic thermohaline circulation in response to increasing atmospheric CO_2 concentration, *Geophys. Res. Lett.*, *32*, L12703, doi:10.1029/2005GL023209.

Körtzinger, A., J. Schimanski, U. Send, and D. W. R. Wallace (2004), The ocean takes a deep breath, *Science*, *306*, 1337.

Lavender, K. L., R. E. Davis, and W. Brechner Owens (2000), Mid-depth recirculation observed in the interior Labrador and Irminger seas by direct velocity measurements, *Nature*, *407*, 66–69.

Lazier, J., R. Hendry, A. Clarke, I. Yashayaev, and P. Rhines (2002), Convection and restratification in the Labrador Sea, 1990–2000, *Deep Sea Res.*, *49*, 1819–1835.

Lee, K., F. J. Millero, and D. M. Campbell (1996), The reliability of the thermodynamic constants for the dissociation of carbonic acid in seawater, *Mar. Chem.*, *55*, 233–245.

Liss, P. S., and L. Merlivat (1986), Air-sea gas exchange rates: introduction and synthesis, in *The Role of Air-Sea Exchange in Geochemical Cycling*, edited by P. Buat-Menard, *NATO ASI Sci. Ser., Ser. C*, *185*, 113–128.

McKinley, G. A., M. J. Follows, and J. Marshall (2004), Mechanisms of air-sea CO_2 flux variability in the equatorial Pacific and the North Atlantic, *Global Biogeochem. Cycles*, *18*, GB2011, doi:10.1029/2003GB002179.

Miller, L. A., et al. (2002), Carbon distributions and fluxes in the North Water, 1998 and 1999, *Deep Sea Res., Part II*, *49*, 5151–5170.

Skjelvan, I., et al. (2005), A review of the inorganic carbon cycle of the Nordic Seas and Barents Sea, in *The Nordic Seas: An Integrated Perspective*, *Geophys. Monogr. Ser.*, vol. 158, edited by H. Drange et al., pp. 157–176, AGU, Washington, D. C.

Tait, V. K., R. M. Gershey, and E. P. Jones (2000), Inorganic carbon in the Labrador Sea: Estimation of the anthropogenic component, *Deep Sea Res., Part I*, *47*, 295–308.

Takahashi, T., et al. (2002), Global sea-air CO_2 flux based on climatological surface ocean pCO_2, and seasonal biological and temperature effects, *Deep Sea Res., Part II*, *49*, 1601–1622.

Tian, R. C., D. Deibel, R. B. Rivkin, and A. F. Vézina (2004), Biogenic carbon and nitrogen export in a deep-convection region: Simulations in the Labrador Sea, *Deep Sea Res., Part I*, *51*, 413–437.

Wanninkhof, R. (1992), Relationship between wind speed and gas exchange over the ocean, *J. Geophys. Res.*, *97*, 7373–7382.

Weiss, R. F. (1974), Carbon dioxide in water and seawater: The solubility of a non-ideal gas, *Mar. Chem.*, *2*, 203–215.

R. G. J. Bellerby, Bjerknes Centre for Climate Research, University of Bergen, N-5007 Bergen, Norway.

M. D. DeGrandpre, Department of Chemistry, University of Montana, Missoula, MT 59812, USA. (michael.degrandpre@umontana.edu)

A. Körtzinger and D. W. R. Wallace, Marine Biogeochemie, Leibniz-Institut für Meereswissenschaften, D-24105, Kiel, Germany.

U. Send, Scripps Institution of Oceanography, University of California, San Diego, La Jolla, CA 92037, USA.